Performance improvement of integrated MEMS/GNSS systems

Jean-Rémi de Boer, Vincent Calmettes, Jean-Yves Tourneret, B. Lesot

Performance Improvement of Integrated MEMS/GNSS Systems

J.-R. De Boer, *Université de Toulouse, ENSEEIHT, IRIT, Toulouse, France*
V. Calmettes, *Université de Toulouse, DEOS, ISAE, TESA, Toulouse, France*
J.-Y. Tourneret, *Université de Toulouse, ENSEEIHT, IRIT, Toulouse, France*
B. Lesot, *Thales Avionics, Valence, France*

BIOGRAPHY

Jean-Rémi De Boer is graduated as an Electronic Engineer from ENSEEIHT (Ecole Nationale Supérieure d'Electrotechnique, d'Electronique, d'Informatique, d'Hydraulique et des Télécommunications) in the university of Toulouse, France. Since September 2006, he has been working on GNSS/MEMS hybridization in the Institut de Recherche en Informatique de Toulouse (IRIT, UMR 5505 of the CNRS) as a PhD student.

Vincent Calmettes received a Ph.D. degree in signal processing from SUPAERO (ISAE), Toulouse, France. He is an engineer researcher in the laboratory of signals, communications, antenna and navigation, at ISAE. His research interests include the development of solutions based on DSP and programmable logic devices or ASICs for applications in Digital communications and Signal processing. He is currently working on new Galileo signal processing and GNSS receiver architectures. He is also involved in several projects devoted to positioning and attitude determination, including low cost MEMS sensors characterization and Inertial Navigation System (INS)/GPS integration.

Jean-Yves Tourneret received the ingénieur degree in electrical engineering from the Ecole Nationale Supérieure d'Electronique, d'Electrotechnique, d'Informatique et d'Hydraulique in Toulouse (ENSEEIHT) in 1989 and the Ph.D. degree from the National Polytechnic Institute from Toulouse in 1992. He is currently a professor in the university of Toulouse, France (ENSEEIHT) and a member of the IRIT laboratory (UMR 5505 of the CNRS). His research activities are centered around statistical signal processing with a particular interest to segmentation, classification and Markov Chain Monte Carlo methods. He was the program chair of the European conference on signal processing (EUSIPCO), which was held in Toulouse (France) in 2002. He was also member of the organizing committee for the international conference ICASSP'06 which was held in Toulouse (France) in 2006. He has been a member of different technical committees including the Signal Processing Theory and Methods (SPTM) committee of the IEEE Signal Processing Society (2001-2007). He is currently an associate editor with the IEEE Transactions on Signal Processing.

Bertrand Lesot graduated from ECN (Nantes, Fr) completed by a research assistantship in Polytechnic University of Montreal, CA. He has joined THALES Avionics research department in 2001 and is working as a lead engineer on design of Inertial/GNSS integrated navigation filters.

ABSTRACT

Inertial Navigation Systems (INS) and Global Navigation Satellite Systems (GNSS) are often combined in vehicle navigation systems to ensure high accuracy navigation. The last generation of Inertial Measurement Unit (IMU) referred to as Micro-Electro-Mechanical Systems (MEMS) might be used in a lot of new applications thanks to their relatively low cost. Unfortunately, the information given by the MEMS are less accurate than with classical INS. This paper studies a two-step inversion procedure which improves the performance of an integrated GNSS/MEMS navigation system. This inversion is based on a good knowledge of the non linear model of the sensor output.

After describing the MEMS models considered in this paper, we present the two steps of the proposed inversion procedure. The goal of the first step (referred to as calibration) is to estimate the model parameters that are related to sensor perturbations. This calibration is performed using the classical least square algorithm which uses the model inputs and outputs. The second step (referred to as model inversion) estimates the model inputs (i.e. acceleration and angular rate) by using an appropriate extended Kalman filter (EKF). Note that the observation equation required for the EKF depends on the estimated parameters resulting from the first step.

The performance of the proposed INS/GPS hybridization is evaluated via several simulations which outline the relevance of the proposed calibration/inversion strategy. These

simulations have allowed to conclude on the accuracy of each step detailed in this paper.

1 INTRODUCTION

Vehicle navigation systems often include an Inertial Measurement Unit (IMU) to bridge GNSS satellite outages (signal blockage, jamming) or GNSS signal degradation (jamming, multipath). Most Inertial Navigation Systems (INS) include accurate but high cost IMUs. Recently, a new generation of inertial sensors called Micro-Electro-Mechanical Systems (MEMS) has become available at relatively low cost. These sensors might be used in many mass-market applications, e.g including land vehicles. However, the performance of these systems is largely dependent upon the quality of inertial sensors. In the case of MEMS, a possible solution for compensating errors due to bias offsets and scale factors is to calibrate the sensor outputs (Syed et al., 2007).

This paper studies an integrated GNSS/MEMS navigation system which takes into account an accurate nonlinear model of the MEMS sensors. The inputs of this model are the vehicle accelerations and the angular rates. The model outputs are the accelerometer and gyroscope measurements. This MEMS model has to be inverted for navigation purposes. However, a fundamental problem during this inversion is that the model parameters are unknown and have to be estimated. The main contribution of this paper is to study a two-step inversion procedure appropriate to MEMS navigation. The first step (referred to as calibration) consists of estimating the model parameters from the system inputs and outputs using a least-squares (LS) estimation method. Note that this LS method uses acceleration and angular rate estimates resulting from GPS measurements. The second step of model inversion consists of estimating the system inputs (accelerations and angular rates) from its outputs (accelerometer/gyroscope outputs). After building an appropriate dynamical model, an extended Kalman filter (EKF) is classically proposed for this estimation.

Once this inversion procedure is achieved, it is also necessary to define a hybridization strategy. This paper considers a GNSS/INS tightly coupled architecture in different kinds of environments. First is described a nominal scenario during which 6 satellites are available all along the trajectory. Then trajectory subjected to a total 30 seconds-long outage is studied. Nominal and total outage scenarios allow to conclude on the accuracy of both cases.

2 MEMS MODELS

As described in Farrell and Barth, 1998, the navigation errors can arise from different sources including instrumentation errors, computational errors, alignment errors and environment errors. Neglecting computational errors, the navigation errors will depend upon the three remaining sources that are due to accelerometer and gyroscope in the case of INS. A very general model for MEMS accelerometers and gyroscopes can be written

$$S = \Phi(\Gamma, \Omega, \theta) \tag{1}$$

where
- S is the MEMS output
- Γ is the true acceleration
- Ω is the true angular rate
- θ is the intrinsic MEMS parameters
- Φ is the MEMS nonlinearity function

The nonlinearity Φ and the parameter vector θ associated to the accelerometer and gyroscope models are detailed in the next sections.

2.1 Accelerometer Model

The accelerometer model considered in this paper contains perturbations due to biases, scale factors, nonlinearities, misalignments and additive noises. It is then defined as follows:

$$S_a = (I - \delta_{SFa} - \delta_{MAa})(\Gamma - \delta_{Ba} - \delta_{NLa} - \upsilon_a) \tag{2}$$

where
- $\Gamma \in \mathbb{R}^3$ is the true acceleration vector.
- $S_a \in \mathbb{R}^3$ is the accelerometer output vector.
- $\delta_{Ba} \in \mathbb{R}^3$ is the vector of bias errors.
- δ_{SFa} is the 3×3 diagonal matrix of scale factor errors.
- $\delta_{NLa} \in \mathbb{R}^3$ is the vector of nonlinearity errors.
- δ_{MAa} is the 3×3 off-diagonal matrix of misalignment errors.
- $\upsilon_a \in \mathbb{R}^3$ is the accelerometer noise vector.

2.2 Gyroscope Model

The gyroscope model contains perturbations due to biases, scale factors, sensitivity to accelerations (g sensitivity), misalignments and additive noises. It can be represented by the following input/output relation:

$$S_g = (I - \delta_{SFg} - \delta_{MAg})(\Omega - \delta_{Bg} - \delta_{Kg} - \upsilon_g) \tag{3}$$

where
- $\Omega \in \mathbb{R}^3$ is the true angular rate vector.
- $S_g \in \mathbb{R}^3$ is the gyroscope output vector.
- $\delta_{Bg} \in \mathbb{R}^3$ is the vector of bias error.
- δ_{SFg} is the 3×3 diagonal matrix of scale factor errors.
- δ_{MAg} is the 3×3 off-diagonal matrix of misalignment errors.
- δ_{Kg} is the 3×3 matrix of uncompensated gyro g sensitivity.
- $\upsilon_g \in \mathbb{R}^3$ is the gyroscope noise vector.

It is interesting to note here that the bias, scale factor and misalignment terms can depend on time and temperature. It has been considered here that onboard compensation can remove thermal effects. As a consequence, errors due to the temperature have not been considered in this paper.

In order to increase the navigation accuracy, we propose to invert the two MEMS models introduced in sections 2.1 and 2.2. A fundamental problem during the inversion step is that the different model parameters are unknown and have to be estimated. The main idea of this paper is to implement a two-step inversion procedure appropriate to navigation with MEMS:

- The first step (referred to as calibration) consists of estimating the model parameters from the system inputs and outputs. This paper proposes to use LS estimation methods for calibration. This first step provides an initial value of the model parameters.

- The second step of model inversion consists of estimating the system inputs (accelerations and angular rates) from its outputs (accelerometer/gyroscope outputs). After building a dynamical system model, we propose to perform this estimation by an appropriate EKF.

3 CALIBRATION

Different strategies can be used to solve the calibration problem for the MEMS models described previously. This paper proposes to estimate the MEMS parameters using the minimum mean squared error (MMSE) principle. This estimation requires to have some coarse values of the model inputs (i.e. accelerations and angular rates). These inputs will be obtained from GPS measurements as illustrated below.

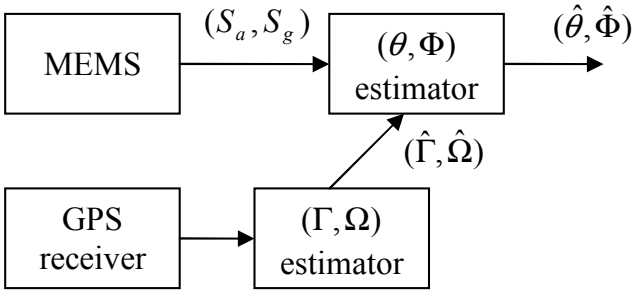

Figure 1. Calibration Step.

The MMSE estimators for the accelerometer and gyroscope parameters are detailed in the following two sections.

3.1 Accelerometer Calibration

With the assumption that nonlinearity is taken into account by a second order polynomial, equation (2) for the accelerometer vector can be written:

$$\begin{pmatrix} S_a^u \\ S_a^v \\ S_a^w \end{pmatrix} = \begin{pmatrix} 1-\delta_{SFa}^u & \delta_{MAa}^{uw} & \delta_{MAa}^{uv} \\ \delta_{MAa}^{vw} & 1-\delta_{SFa}^v & \delta_{MAa}^{vu} \\ \delta_{MAa}^{wv} & \delta_{MAa}^{wu} & 1-\delta_{SFa}^w \end{pmatrix} \times \begin{pmatrix} \Gamma^u - \delta_{Ba}^u - \delta_{NL2a}^u (\Gamma^u)^2 - \upsilon_a^u \\ \Gamma^v - \delta_{Ba}^v - \delta_{NL2a}^v (\Gamma^v)^2 - \upsilon_a^v \\ \Gamma^w - \delta_{Ba}^w - \delta_{NL2a}^w (\Gamma^w)^2 - \upsilon_a^w \end{pmatrix}$$

where u, v and w are the 3 accelerometer axis defined in Farrell and Barth, 1998. As a consequence, by neglecting the cumulated effect of two perturbations, the first accelerometer component expresses as

$$\begin{aligned} S_a^u = \quad & (1-\delta_{SFa}^u)\Gamma^u + \delta_{MAa}^{uw}\Gamma^v + \delta_{MAa}^{uv}\Gamma^w \\ & \cdots - \delta_{Ba}^u - \delta_{NL2a}^u (\Gamma^u)^2 - \upsilon_a^u \end{aligned} \tag{4}$$

or equivalently

$$S_a^u = \underbrace{\begin{pmatrix} 1 & \Gamma^u & \Gamma^v & \Gamma^w & (\Gamma^u)^2 \end{pmatrix}}_{G} \underbrace{\begin{pmatrix} -\delta_{Ba}^u \\ 1-\delta_{SFa}^u \\ \delta_{MAa}^{uw} \\ \delta_{MAa}^{uv} \\ \delta_{NL2a}^u \end{pmatrix}}_{Z} - \upsilon_a^u.$$

This last equation is linear in the unknown parameter vector Z. As a consequence, the MMSE estimator of Z can be written

$$\hat{Z}_{MMSE} = (G^T G)^{-1} G^T S_a^u. \tag{5}$$

Similar derivations for the accelerometer parameters associated to the axes v and w are straightforward and are omitted here for brevity.

3.2 Gyroscope Calibration

With the assumption that g sensitivity is taken into account by a first order polynomial, equation (3) for the gyroscope vector can be written:

$$\begin{pmatrix} S_g^p \\ S_g^q \\ S_g^r \end{pmatrix} = \begin{pmatrix} 1-\delta_{SFg}^p & \delta_{MAg}^{pr} & \delta_{MAg}^{pq} \\ \delta_{MAg}^{qr} & 1-\delta_{SFg}^q & \delta_{MAg}^{qp} \\ \delta_{MAg}^{rq} & \delta_{MAg}^{rp} & 1-\delta_{SFg}^r \end{pmatrix} \times \begin{pmatrix} \Omega^p - \delta_{Bg}^p - \delta_{Kg}^{pu}\Gamma^u - \delta_{Kg}^{pv}\Gamma^v - \delta_{Kg}^{pw}\Gamma^w - \upsilon_g^p \\ \Omega^q - \delta_{Bg}^q - \delta_{Kg}^{qu}\Gamma^u - \delta_{Kg}^{qv}\Gamma^v - \delta_{Kg}^{qw}\Gamma^w - \upsilon_g^q \\ \Omega^r - \delta_{Bg}^r - \delta_{Kg}^{ru}\Gamma^u - \delta_{Kg}^{rv}\Gamma^v - \delta_{Kg}^{rw}\Gamma^w - \upsilon_g^r \end{pmatrix}$$

where p, q and r are the 3 gyroscope axis defined in Farrell and Barth, 1998. By neglecting the cumulated effect of two perturbations, the first gyroscope component expresses as

$$\begin{aligned} S_g^p = \quad & (1-\delta_{SFg}^p)\Omega^p + \delta_{MAg}^{pr}\Omega^q + \delta_{MAg}^{pq}\Omega^r - \delta_{Bg}^p \\ & \cdots - \delta_{Kg}^{pu}\Gamma^u - \delta_{Kg}^{pv}\Gamma^v - \delta_{Kg}^{pw}\Gamma^w - \upsilon_g^p \end{aligned} \tag{6}$$

or equivalently

$$S_g^p = \underbrace{\begin{pmatrix} 1 & \Omega^p & \Omega^q & \Omega^r & \\ & \cdots & \Gamma^u & \Gamma^v & \Gamma^w \end{pmatrix}}_{O} \underbrace{\begin{pmatrix} -\delta_{Bg}^p \\ 1-\delta_{SFg}^p \\ \delta_{MAg}^{pr} \\ \delta_{MAg}^{pq} \\ \delta_{Kg}^{pu} \\ \delta_{Kg}^{pv} \\ \delta_{Kg}^{pw} \end{pmatrix}}_{Y} - \upsilon_g^p.$$

This last equation is linear in the unknown parameter vector Y. As a consequence, the MMSE estimator of Y can be written

$$\hat{Y}_{MMSE} = (O^T O)^{-1} O^T S_g^p. \tag{7}$$

Similar derivations for the gyroscope parameters associated to the axes v and w are straightforward and are omitted here for brevity.

4 MODEL INVERSION

As explained before, model inversion consists of estimating the MEMS inputs (i.e. accelerations and angular rates) from the MEMS outputs. This operation is illustrated in Fig. 2. The classical idea considered in this paper is to model the dynamics of the acceleration and angular rate by random walks. The state space representation associated to this random walk model is summarized below

$$\begin{cases} \Gamma_k = \Gamma_{k-1} + \upsilon_{\Gamma,k} \\ \Omega_k = \Omega_{k-1} + \upsilon_{\Omega,k} \\ S_k = \Phi(\Gamma_k, \Omega_k, \theta_k) + \upsilon_{S,k} \end{cases} \tag{8}$$

where υ_Γ and υ_Ω are additive white Gaussian noises whose variances have been selected to high values in order to ensure possible high dynamic motions. The estimation of the acceleration and angular rate vectors Γ_k and Ω_k is achieved using two EKFs based on state space equations detailed in the following sections.

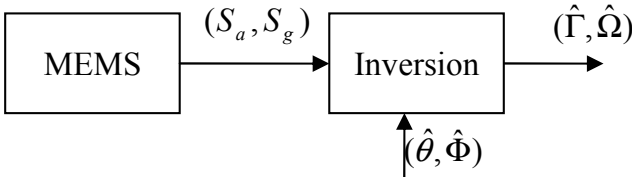

Figure 2. Inversion Step.

4.1 Accelerometer Model Inversion

The state space equations associated to the estimation of the acceleration vector are

$$\begin{cases} \Gamma_k = \Gamma_{k-1} + \upsilon_{\Gamma,k} \\ S_{a,k} = \Phi_a(\Gamma_k, \hat{Z}_{MMSE}) + \upsilon_{a,k} \end{cases} \tag{9}$$

where Γ_k contains the 3 accelerations components associated to the axes u, v and w.

4.2 Gyroscope Model Inversion

The angular rates are estimated conditionally upon the previously estimated accelerations. The corresponding state space equations can be written

$$\begin{cases} \Omega_k = \Omega_{k-1} + \upsilon_{\Omega,k} \\ S_{g,k} = \Phi_g(\Omega_k, \hat{\Gamma}_k, \hat{Y}_{MMSE}) + \upsilon_{g,k} \end{cases} \tag{10}$$

where Φ_g contains the 3 angular rate components associated to the axes p, q and r.

5 SIMULATION RESULTS

This section presents simulation results for the estimation of the MEMS model parameters, accelerations and angular rates. Appropriate models for the biases and scales factors have been provided by Thales Avionics and are omitted here for confidentiality reasons.

5.1 Calibration

All calibration results shown in this section have been averaged from 1000 Monte Carlo runs. Moreover, 50 random values of the parameters have been considered in each simulation. Figures 3, 4, 5 and 6 show the mean square errors (MSEs) respectively for biases, scale factors, misalignments and second order terms for the non-linearity. First, it is important to mention here that the orders of magnitude of the different parameters are approximately 10^{-2} for δ_{Ba} and δ_{MAa}, and 10^{-5} for δ_{SFa} and δ_{NL2a}. Figures 3 and 5 show that calibration results are very good for biases and misalignments. The calibration procedure is less efficient for scale factors and second order nonlinearity terms as depicted in figures 4 and 6.

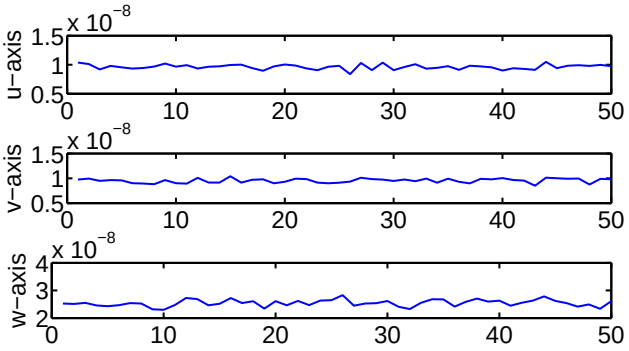

Figure 3. MSE of δ_{Ba}.

The next simulation results are related to the gyroscope parameters. Figures 7, 8, 9 and 10 correspond to the biases, scale factors, misalignments relatively to p-axis and uncompensated gyro g sensitivity relatively to u-axis. The orders of magnitude for these parameters are approximately 10^{-2} for δ_{Bg} and δ_{MAg}, 10^{-4} for δ_{SFg}, and 10^{-3} for δ_{Kg}. The results obtained in 7, 8 and 9 are good in term of calibration. Conversely, the uncompensated gyro g sensitivity is estimated with less efficiency as depicted in Fig. 10.

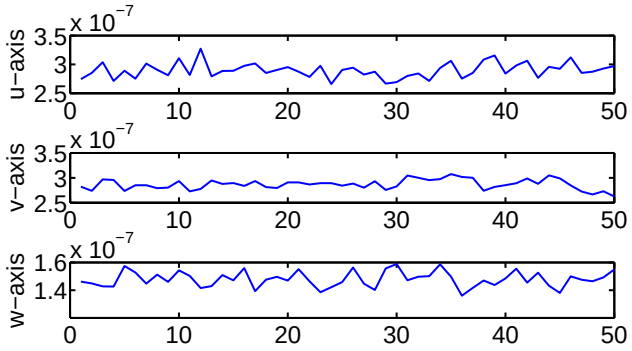

Figure 4. MSE of δ_{SFa}.

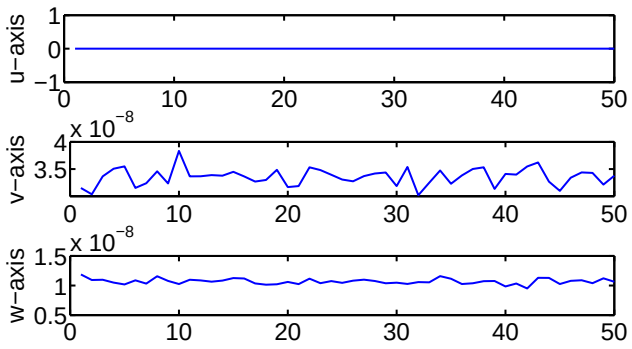

Figure 5. MSE of $\delta^{u.}_{MAa}$.

5.2 Model Inversion

The model inversion results have been averaged from 300 Monte Carlo runs. Each mean square error has been estimated using a random trajectory of 120 seconds. Figures 11 and 12 show the acceleration and angular rate MSEs. Then the obtained accuracy is approximately $10^{-5}g^2$ and $10^{-3}(^\circ/s)^2$ for these two parameter vectors.

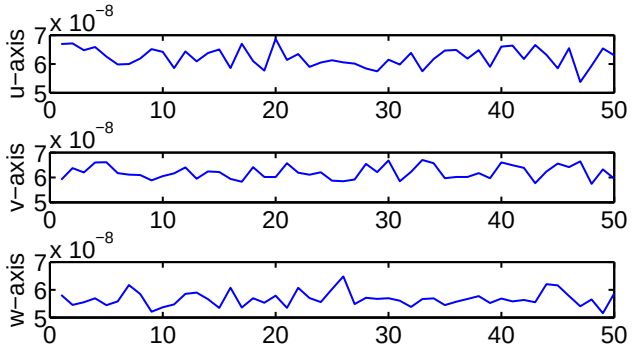

Figure 6. MSE of δ_{NL2a}.

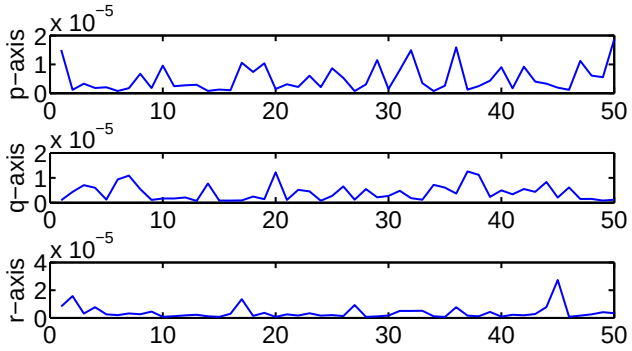

Figure 7. MSE of δ_{Bg}.

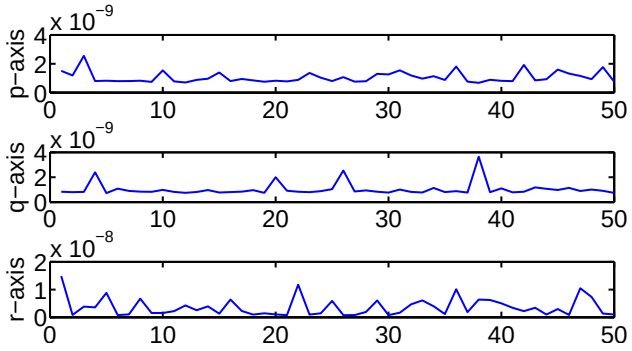

Figure 8. MSE of δ_{SFg}.

5.3 Navigation

The complementarity of GNSS and INS systems has been used efficiently in many applications. Short-term position errors of INS are relatively small but degrade without remaining bounded over the time whereas GNSS errors do not degrade with time but are more important during a short period. Many different integration architectures have been proposed in the literature [Farrell and Barth, 1998; Grewal et al., 2007]. This paper considers a tightly coupled archi-

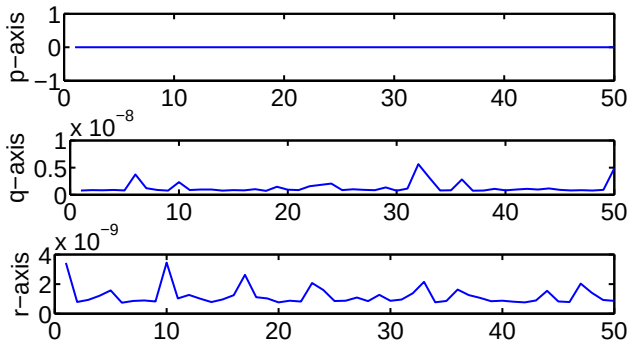

Figure 9. MSE of $\delta^{p.}_{MAg}$.

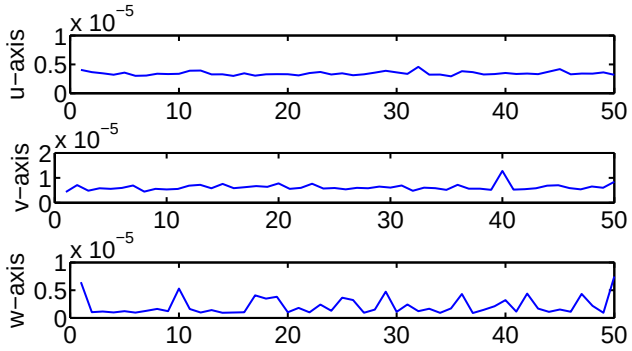

Figure 10. MSE of $\delta^{p.}_{Kg}$.

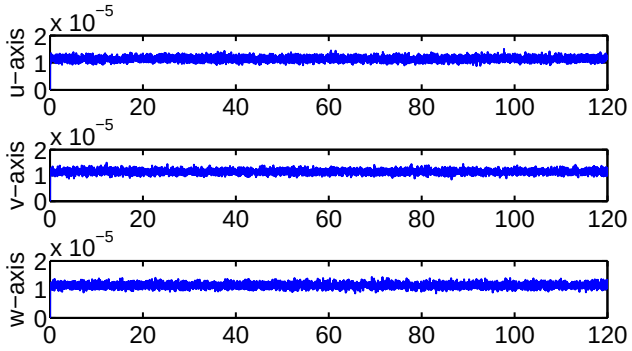

Figure 11. MSE of $\Gamma[g^2]$.

tecture for GPS/INS hybridization as described in Giremus, 2005 and Priot et al., 2008 and summarized in Fig. 13. This section will compare navigation results obtained with a good quality IMU (considered as a reference and denoted as "INS") and a lower quality IMU based on MEMS (denoted as "Calibrated MEMS" or "MEMS" depending on whether calibration has been used or not).
The state vector associated to this architecture is estimated using a classical EKF. This paper focuses on two different experimentations described below. All figures have been

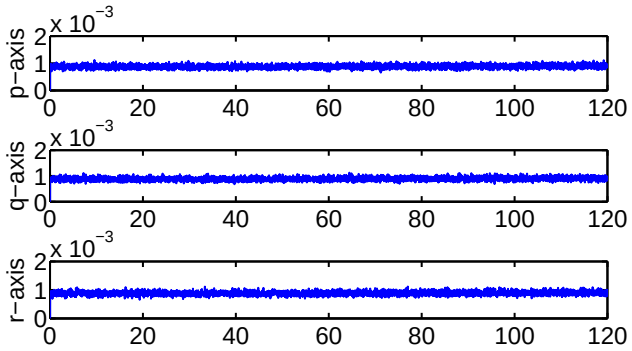

Figure 12. MSE of $\Omega[(^\circ/s)^2]$.

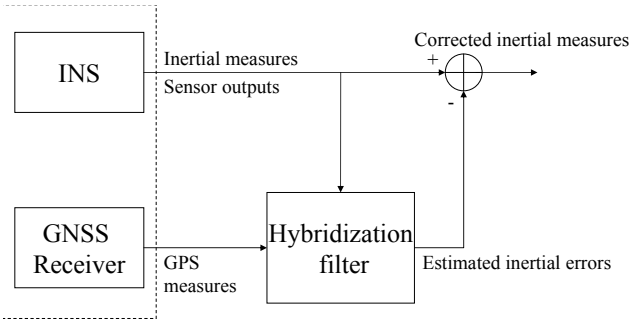

Figure 13. Hybridization architecture.

obtained by averaging 200 Monte Carlo runs and the estimates have been computed using random trajectories of 600 seconds.

5.3.1 Experiment 1

The first experiment is a nominal scenario during which 6 satellites are available all along the trajectory. Figures 14 and 15 show the averaged norms of the estimates as well as plus and minus standard deviation bands. The calibration procedure clearly improves the navigation performance especially during the first 150 seconds (assuming calibration has been achieved at time $t = 0s$). Moreover, the hybridization between GPS and calibrated MEMS tends to perform similarly to the usual GPS/INS coupling. This is a very encouraging result.

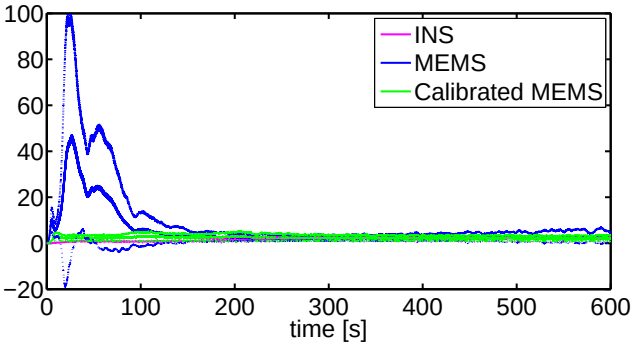

Figure 14. MEMS/GPS position error without outage $[m]$.

5.3.2 Experiment 2

The second experiment considers a trajectory subjected to a total outage of 30 seconds (out of the 600 seconds). Figures 16, 17 and 18 show the averaged norms of the estimates as well as plus and minus standard deviation bands during different time intervals. The good performance of the proposed GPS/calibrated MEMS hybridization is confirmed when GPS measurements are available. However,

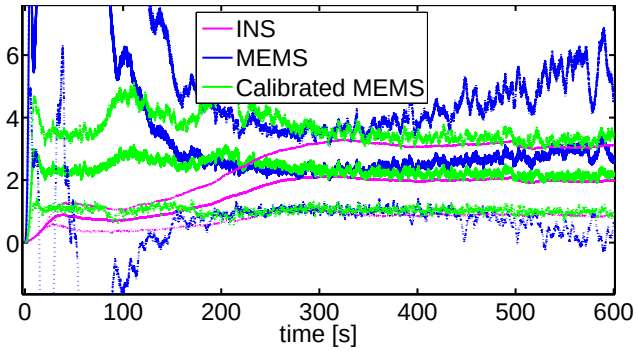

Figure 15. MEMS/GPS position error without outage [m] (zoom).

the performance of this hybridization is limited (when compared to the usual GPS/INS hybridization) in presence of GPS outage. In fact, the position drift is mainly due to the integration with time of the IMU noises. These noises are larger in the case of MEMS as in the classical INS case and that explains the difference in term of accuracy.

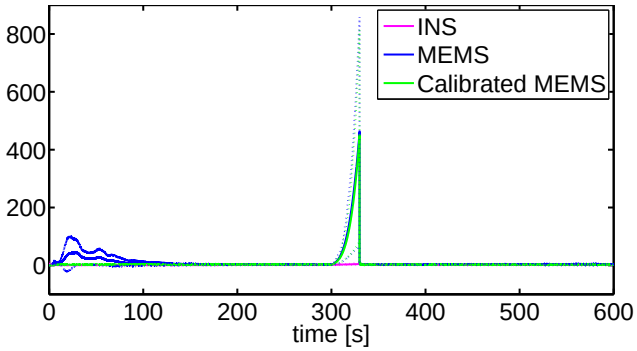

Figure 16. MEMS/GPS position error with outage [m].

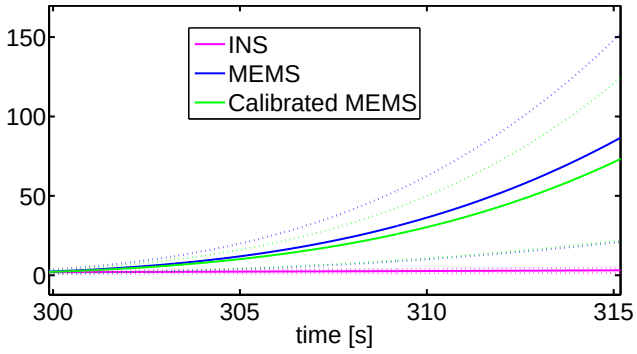

Figure 17. MEMS/GPS position error with outage [m] (zoom on the outage first 15 sec).

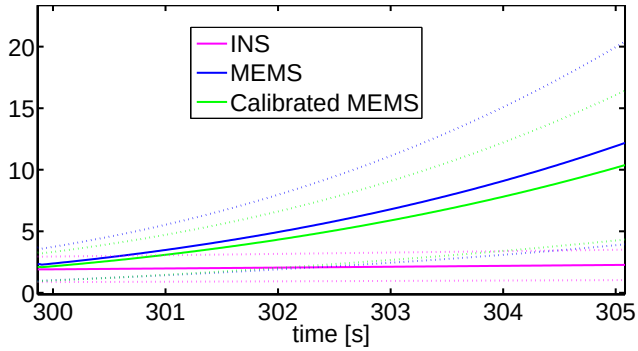

Figure 18. MEMS/GPS position error with outage [m] (zoom on the outage first 5 sec).

6 CONCLUSION

Current progress in MEMS technology has made possible the use of inertial sensors for low cost mass market applications. However, the performance of a GNSS/MEMS system are closely related to the IMU quality, especially during critical navigation scenarios. These scenarios include urban canyon characterized by partial satellite outage and poor geometric dilution of precision (GDOP), and total satellite outage. This paper proposed an approach to improve the quality of MEMS based navigation systems by using calibration.

The calibration strategy studied in this paper was based on a two-step inversion procedure appropriate to navigation with MEMS. First, the model parameters were estimated from system inputs (resulting from GPS measurements) and outputs using least-squares estimation methods. Second, model inversion was used to estimate the accelerations and angular rates from accelerometer/gyroscope outputs. Simulations results illustrated the performance of the proposed navigation strategy and especially the GPS outage case during which the improvements are light.

Progresses in MEMS technology should continue in the future decade and might lead to high accuracy navigation systems. Our future investigations include the development of new GPS/MEMS architectures which are more robust to GPS outages and should be based on learning method such as neural network.

ACKNOWLEDGEMENTS

The authors would like to thank DGA and Thales Avionics for supporting this work.

REFERENCES

Farrell, J. and Barth, M. (1998). *The Global Positioning System & Inertial Navigation.* McGraw-Hill.

Giremus, A. (2005). *Apports des techniques de filtrage non linéaire pour la navigation avec les systèmes de navi-*

gation inertiels et le GPS. PhD thesis, Ecole Nationale Supérieure de l'Aéronautique et de l'Espace.

Grewal, M., Weill, L., and Andrews, A. (2007). *Global Positioning System, Inertial Navigation, and Integration*. John Wiley & Sons, second edition.

Priot, B., De Boer, J.-R., Guidoux, R., and Calmettes, V. (2008). Performance assessment of integrated MEMS/GNSS systems. *Proc. of ENC-GNSS*.

Syed, Z., Aggarwal, P., Goodall, C., Niu, X., and El-Sheimy, N. (2007). A new multi-position calibration method for mems inertial navigation systems. *Measurement Science and Technology*, Volume 18(Number 7):pp. 1897–1907.